Mathematical Statistician and Engineering Applications
ISSN: 2094-0343
2326-9865

Analysis of CNN and Quantized CNN Model's Performance for Osteoarthritis Identification

[1]Sivaprasad Lebaka, Research Scholar, Department of Electronics and Communication Engineering, Visvesvaraya Technological University, Belagavi, Karnataka, India
Corresponding author E-mail: sivaprasadlebaka@gmail.com
[2] Dr. D. G. Anand, Rector - Research, Rajiv Gandhi Institute of Technology, Bengaluru, India
E-mail: dga.ece.rgit@gmail.com

Article Info
Page Number: 1745 – 1759
Publication Issue:
Vol. 71 No. 3s2 (2022)

Article History
Article Received: 22 April 2022
Revised: 10 May 2022
Accepted: 15 June 2022
Publication: 19 July 2022

Abstract-- Aging populations have made osteoarthritis (OA) a serious worldwide health problem. Radiography, Computed Tomography (CT), ultrasonic, Magnetic Resonance Imaging (MRI), and thermal imaging are all utilized to discover and diagnose OA. Early OA may be detected by non-invasive, radiation-free, quick, and accurate infrared (IR) thermal imaging. OA screening may benefit from IR thermography since it gives useful details on the temperature and vascular status of the joints. Thermal imaging for the detection of OA disorders sometimes requires hand analysis and interpretation, which strongly relies on the clinical expertise of the examining physician. The goal of the paper is to automate the OA screening using IR thermographic images. In this study, the required dataset is collected using the IR imaging method. The collected dataset consists of normal and arthritis-affected thermal images. The dataset is then prepared to be compatible with the Convolution Neural Network (CNN) of the Deep Learning (DL) model and statistical parameters such as mean, mode, mode, kurtosis, etc. are derived and the correlation between the parameters is drawn using the covariance matrix. The dataset is then visualized using graphical plots to view the distribution of the statistical parameters. The dataset is then pre-processed using the normalization method and then analyzed using the CNN model. To find the efficiency of the DL model performance metrics such as accuracy, precision, loss, F-1 score, recall, etc. are calculated. To reduce the complexity and to reduce the computational time, the dataset is quantized using the optimization method and a comparison between the trained model and the quantized model is drawn.

I. Introduction

OA is a prevalent condition that ranks as the fourth biggest cause of disability globally [1]. According to the US National Health Survey, up to 14M Americans suffer from knee problems. Taking into account healthcare expenditures and productivity losses, it is estimated that the economic burden associated with OA would equal up to 2.5 percent of Western nations' GDP growth. The current method of treatment for OA, which comprises therapies, has minimal impact on function and pain. OA is one of the most prevalent destructive musculoskeletal illnesses. The knee joint is most frequently affected by OA, which is defined by the irreversible deterioration of articular cartilage at the ends of bones such as the tibial, patella cartilages, and femoral [2]. Knee osteoarthritis (KOA) is a degenerative condition that affects the whole knee joint. KOA is produced by both severe wear and tear and metabolic alterations. Age, obesity and a history of knee injury are all recognized risk factors for OA. OA results in pain, which impairs function and diminishes the quality of life. The joint degeneration caused by OA is permanent, and the only treatment option is total knee

replacement (TKR), which is costly and has a limited life expectancy, particularly in obese patients. Therefore, early recognition of KOA is essential for commencing treatment, such as weight reduction and exercise, which help prevent KOA development and extend TKR. Consequently, there is a substantial unmet medical need for a disease-modifying osteoarthritis drug (DMOAD) that may halt disease development and lessen the need for knee surgery. The development of such DMOADs is now unsuccessful. There are considerable variances between people in the course of cartilage degradation [3]. Osteoarthritis is a disorder wherein the cartilage in one or more of the body's joints progressively deteriorates. This condition may make it difficult to walk and do ordinary chores such as playing a musical instrument. Traditionally, X-ray images were used to support the diagnosis depending on a person's illness. Figure 1 shows how researchers used thermal imaging of knee joints to obtain insights into the inflammation phases of osteoarthritis.

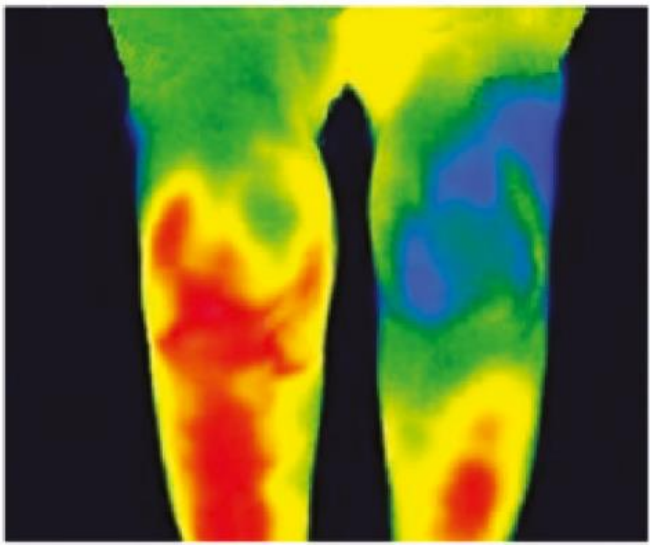

Fig. 1 Thermal image of knee joints

Various imaging modalities are utilized to diagnose OA. X-rays are the most reliable method for identifying joint degeneration and displacement in OA patients [4-6]. MRI gives 3D images of the RA-affected joints, whereas radiography produces only 2D images. MRIs and ultrasounds, for instance, can be utilized to determine the severity of OA [7]. Thermal imaging is regarded as a quick and premature detection method for OA disease assessment. Numerous benefits accompany the use of thermal imaging techniques in the early detection of OA issues. These are non-invasive, radiation-free, non-contact, and non-invasive. Few researchers focused on employing thermal imaging to monitor and diagnose OA. This IR thermography imaging method [8] is entirely risk-free.

II. Related Works

Since OA is a long-term illness, there is plenty of time to affect its progression. Mechanical stress, obesity, and joint injury are all risk factors for OA that have been related to the disease's onset. In the late stages of osteoarthritis, the treatment choices are limited. Radiographic joint-space narrowing, which has been used to diagnose OA for millennia, is an

extremely insensitive approach. With optical and MRI advancements, direct imaging of joint tissues is now available, allowing for a quantitative assessment of joint tissue structure to identify early OA [9]. Aside from that, MRIs need that patient to stay in the scanner for an extended amount of time. This may be embarrassing at times. X-ray and CT scanners absorb trace quantities of radiation. IRT is a kind of functional imaging that detects heat released at a depth of 1–2 millimeters below the skin's surface using infrared radiation. These clinical applications include the use of infrared thermal imaging to monitor skin temperature increases for pain evaluation [10], the investigation of rheumatoid arthritis (RA) [11,12], hand osteoarthritis [13], and knee osteoarthritis [14,15]. Research [16] uses artificial neural networks and infrared image processing for early prediction. There are many stages in this method. You may begin processing the thermal image after it has been imported into the MATLAB-created GUI. Then, click on the affected region. The system will scan the pixels in a specific region and calculate the temperature based on the color of the pixels in thermal images. When there is inflammation, WBC chemicals are released into the circulation. The release of chemicals that promote blood flow to the site of injury or sickness may cause redness and warmth. The Backpropagation method will be utilized to create an early temperature prediction. Based on radiographs, the Ahlbäck grading system is employed in a computer-aided diagnostic procedure [17] to determine the severity of KOA. The minimum joint space width is used to evaluate the loss of articular cartilage and to classify OA into separate categories. Several supervised classifiers are tested on the Osteoarthritis initiative data set. K Nearest Neighbor produces the most accurate results. When compared to existing methodologies, the proposed strategy has a 97 percent accuracy rate, according to the statistics.

The researchers want to develop a device capable of predicting the progression of pain in KOA-affected persons based on their beginning health state. [18] Using a feature important voting process and machine learning (ML) methods, it is possible to forecast whether KOA discomfort will increase or decrease over time. Considering the low number of characteristics, these models have an overall accuracy of 84.3 percent over a range of subsets of features. Future KOA prevention strategies might be aided by the proposed method's capacity to detect discomfort at an initial point. As part of the work [19], automated KOA classification algorithms depending on the Kellgren-Lawrence grading system, gait analysis, and radiographic imaging data were constructed. Multi-classification of KOA has relied on gait features associated with radiological severity and radiographic imaging variables generated by a DL model. Using just radiographic images as input, the proposed model surpassed a more typical DL technique. By combining gait data and radiographic imaging, computerized detection of multiclass KOA could be enhanced. This research used a deep Siamese Convolutional Neural Network (CNN) with unsupervised LCM segmentation to generate a novel automatic classification of KOA images [20]. Utilizing first-order statistics and a gray-level co-occurrence matrix, the anatomical characteristics of segmented images are retrieved. Just on-premise on the clinical evidence, the network can be trained over seventy-five iterations with automated weight adjustments. Using LCM-segmented KOA images, the suggested network accurately identified KOA. In the literature, thermal imaging had shown to be a non-invasive method for examining physiological processes associated

with fluctuations in body temperature. Thermal imaging analyses variations in skin temperature without the use of damaging radiation to detect early signs of OA. Incorporating thermal imaging into the development of effective technologies is an attractive opportunity. The cost of thermal imaging investigation is cheaper than that of MRI analysis.

III. Materials and Methods

In this study, the required dataset for this work is collected in real-time rather than collecting it from an online repository. To collect the dataset a method called IR imaging is used. Using an IR camera module, the thermal images of the ankle joints are captured. The dataset contains both normal and arthritis-affected thermal images. The collected images are then prepared to make them compatible with the DL model. Significant statistical parameters such as mean, median, mode, etc. for the temperature value are calculated. The prepared data is then visualized to graphically view the distribution of statistical parameters. Then the covariance matrix for the variables is derived. The dataset is then pre-processed using the normalization methods. The pre-processed dataset is then divided into two parts: The training set which is 85% of the total dataset and the validation set which is 15% of the total dataset. The CNN model is then trained using the training dataset and then validated using the validation dataset. The performance metrics such as accuracy, precision, etc. are calculated for the DL model to analyse its efficiency. The dataset is then quantized to reduce complexity and to reduce computation time and the dataset is again validated using the CNN model.

a. Image dataset

The image dataset required for this study is collected in real-time using the IR imaging technique rather than collecting it from some repository available on the internet. The temperature of a specimen is measured using IR imaging methods. Most things emit electromagnetic radiation, especially in the IR range of wavelength, that is invisible to the human eye. IR rays, on the other hand, could be sensed as heat on the epidermis. The more the IR radiation a thing radiates, the warmer it is. There are numerous IR imaging implications in the world of medicine, both for man and livestock. IR thermography is now being employed in thermal imaging to make a diagnosis sooner, identify the root of arthritis, and sometimes even discover circulatory abnormalities before they get too serious. In this study, the IR imaging technique is used to evaluate variations in joint temperature. Using an IR camera thermal images are captured which helps in detecting heat patterns to detect the variation of heat in the joints and may also pinpoint the area of inflammation in the joints.

b. Preparation of the dataset

Figure 2 given above shows the steps involved in the preparation of the image dataset. The thermal images acquired from the thermal camera are then prepared to make them compatible with the CNN model. Each pixel in that thermal image indicates the temperature at that corresponding point. For each image in the dataset value of the attributes [21] such as maximum, minimum mean, median, skewness, mode, kurtosis, and SD of the temperature are evaluated. The parameters that have been processed are saved in Comma-Separated Values (CSV) files, which enables data to be retained in a tabulated manner. The dataset collected contains both normal thermal images and arthritis-affected thermal images. Each entry is labelled 1 for arthritis-affected thermal images and 0 for the normal thermal images.

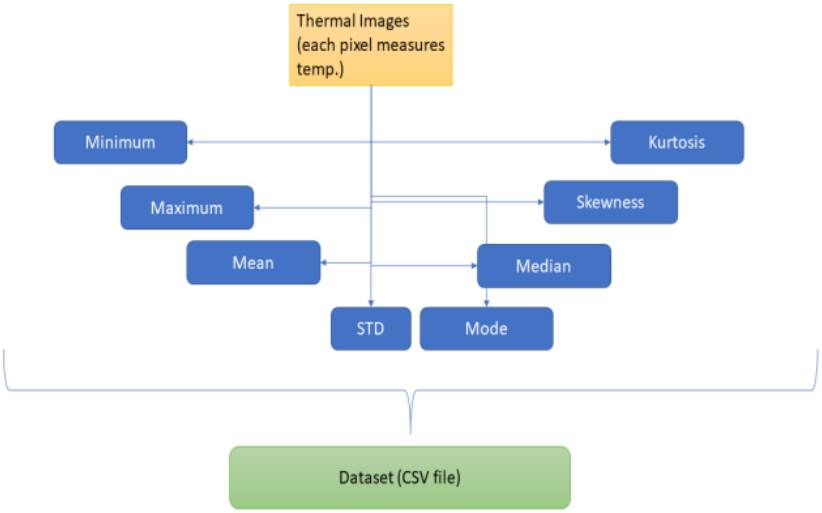

Fig.2 Image preparation steps

c. Data Visualisation

It is a common term for visual representations of statistical data. To make it easier to see and understand statistics and variances in the form of graphs, charts, or maps, visualization tools are used. Each attribute calculated in this study is distributed in a graphical representation in Figure 3, which can see below.

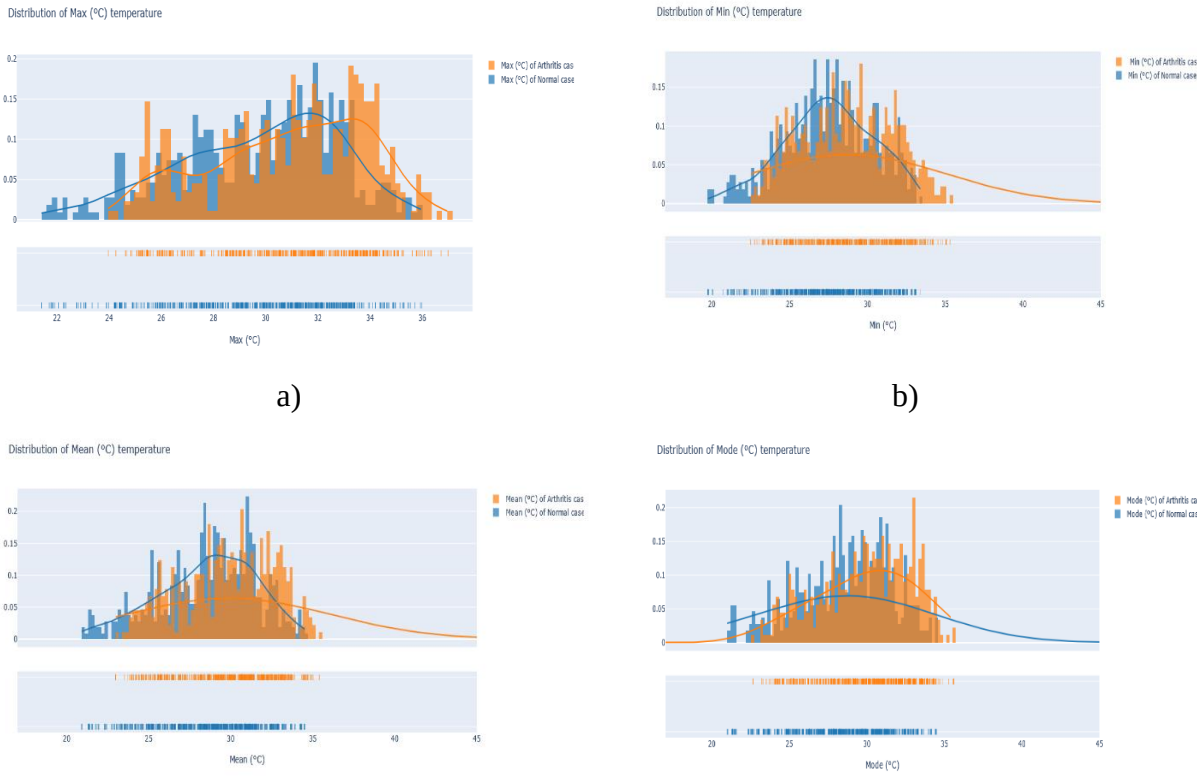

a) b)

c) d)

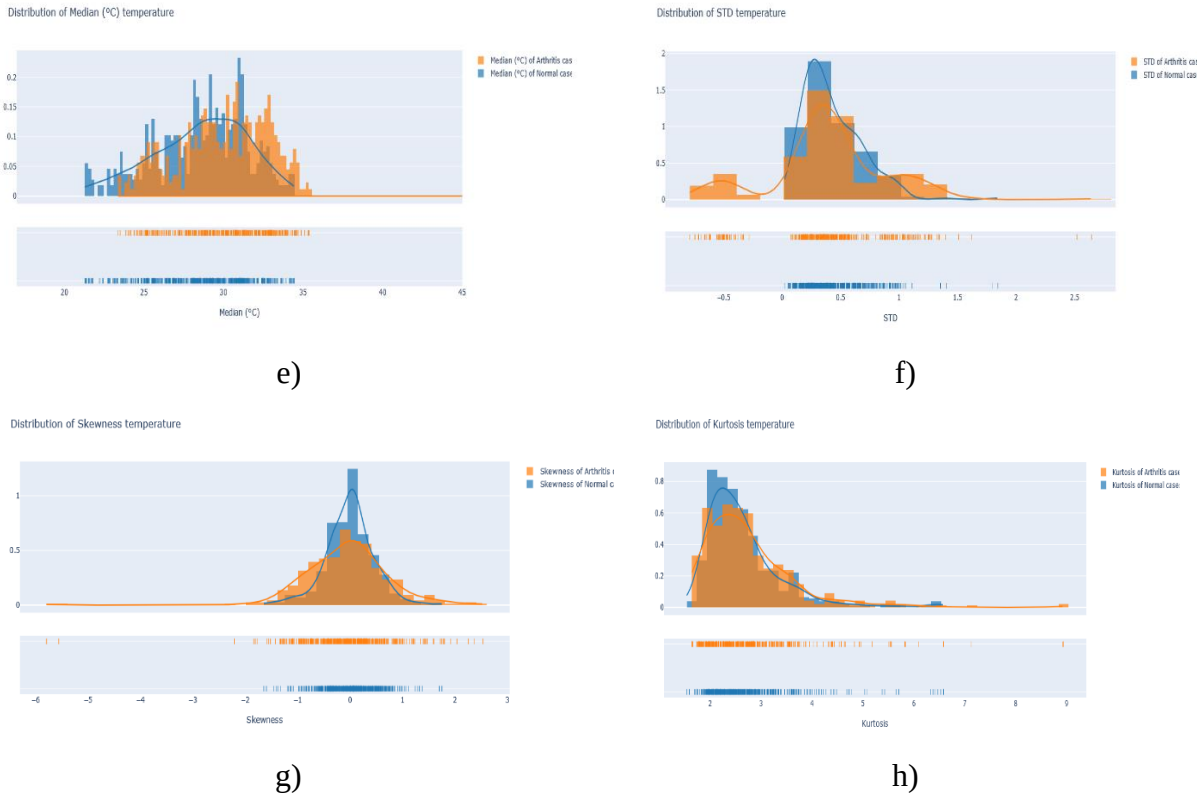

Fig.3 Distribution of statistical parameter

Figure 3 given above shows the graphical representation of the distribution of the statistical parameters calculated such as mean, median, mode, etc. in this study. Figure 3.a shows the graph of Maximum temperature shown by both normal thermal images and arthritis-affected thermal images. Figure 3.b indicates the minimum temperature shown by both normal thermal images and arthritis-affected thermal images. Figure 3.c indicates the mean of the temperature shown by both normal and arthritis-affected thermal images. Figure 3.d depicts the graphical distribution of the mode of the temperature of both normal and arthritis-affected thermal images. Figure 3.e indicates the median temperature of both normal and arthritis-affected thermal images. Figure 3.f illustrates the SD of the temperature of both normal and arthritis-affected thermal images. Figure 3.g represents the distribution of Skewness of the temperature of both normal and arthritis-affected thermal images. Figure 3.h represents the distribution of Kurtosis of the temperature of both normal and arthritis affected thermal images.

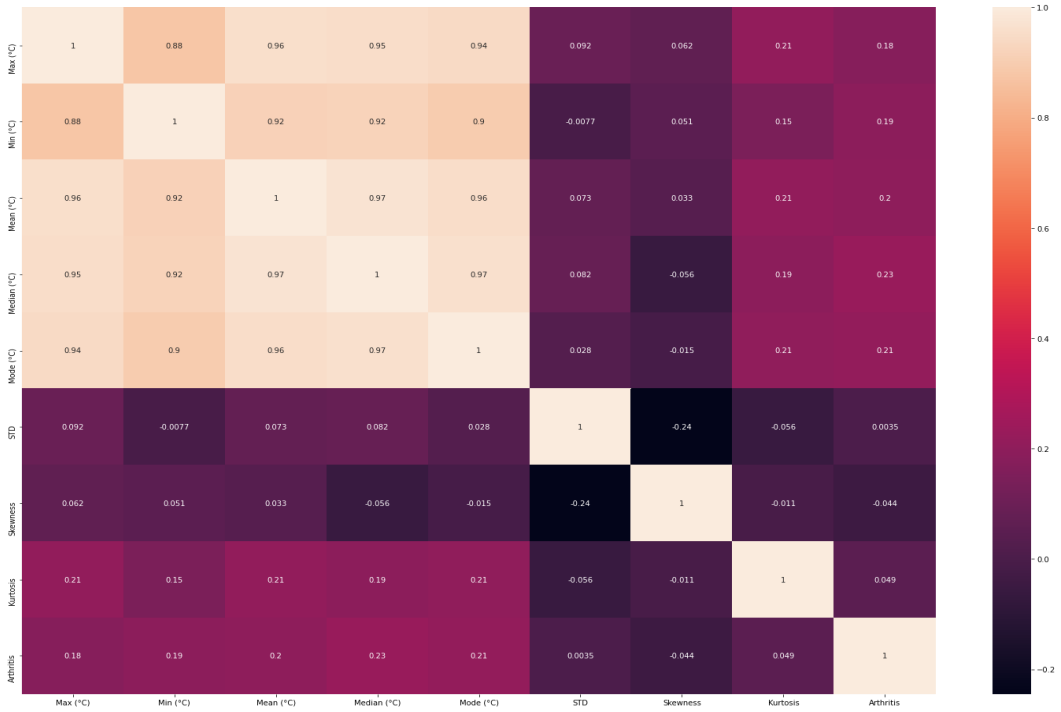

Fig. 4 Covariance Matrix

Figure 4 given above shows the covariance matrix derived for the statistical parameters to find the correlation between the parameters. A covariance matrix is a square matrix that represents the correlation amongst each set of elements in a random vector. It is observed that the variables mean, median, mode, min, and max are highly correlated to each other.

d. Data pre-processing

Normalization is a pre-processing technique in which the data is either scaled or altered such that each characteristic contributes an equal amount to the final output. For ML algorithms to be successful, they must be able to build generalised predictive models of the categorization issue. The significance of data normalisation in enhancing the quality of data and, as a result, the effectiveness of AI algorithms [22]. Normalization is the process of reorganizing data from a database so that it fulfils two fundamental requirements. There is no replication; each piece of data resides in a centralized location. Data dependencies are rational in the sense that all relevant data are maintained collectively. In this study, mean normalization is done on the dataset so that the mean and SD become 0 and 1 correspondingly for every attribute. This leads to a smooth loss curve making it easier for convergence. It also counters the problems like vanishing gradient and exploding gradient.

Mean Normalization is given by, $x_i = \frac{x_i - \mu_i}{s_i}$

Where μ(i) → average values for a feature and *s(i)* → minimum and maximum range of values

e. DL model

As the name implies, neural networks (NN) are a collection of algorithms that handle enormous amounts of data in a manner comparable to that of the brain. A "NN" is a group of neurons that might be biological or synthetic. DL is a form of ML approach that employs interconnected networks of neurons in a layered architecture that mimics the operation of the

human brain. Using NN, which imitates human brain behaviour, computer algorithms may recognize patterns and solve complex problems in AI, computer vision, and DL. A basic NN is divided and distinguished by an input layer, an output layer, and a hidden layer. The various layers are linked together via a "network" of nodes. The CNN design, which includes an input (IL), hidden (HL), and output layers (OL), is used in this work. Images are presented at the IL, and relevant features are taught to HL, with the results obtained at the output layers [23]. The CNN design consists of many convolution layers (CL), a pooling layer (PL), and an activation layer (AL). The CNN's CL is crucial in the feature extraction process. Convolution filters may recognize different features at different levels by altering the kernel size of various filters on the images. PL lower the complexity of the following layers, resulting in a reduction in network parameters. The pooling layer is implemented using nonlinear pooling functions such as average and maximum pooling. In a ReLU, all values lower than zero are mapped to zero, but all values greater than zero are maintained.

Table.1 Network structure

Layer (type)	Output Shape	Parameters
dense_93 (Dense)	(None, 24)	216
dense_93 (Dense)	(None, 12)	300
dense_93 (Dense)	(None, 1)	13

From table 1, it is shown that the number of parameters available in the first dense layer is about 216. The number of parameters present in the second dense layer is about 300 and the number of parameters in the third layer is about 13. The total number of parameters present in this study is about 529 and the number of trainable parameters is about 529 which makes the non-trainable parameters 0.

The dataset has been split into training and validation samples. 85% were used for training purposes and the remaining 15% were used for validation purposes. Mean normalization is performed on the dataset based on the mean and SD of the training dataset. The normalized dataset is used as a training dataset. To Counter, the class imbalance problem weighted binary cross-entropy is used. Where the loss, is weighted for each class based on their ratio in the training dataset. This helped in reducing the loss by a certain amount helping to avoid misclassifications of positive examples. Adam optimizer is used in training and trained for different epochs until the optimal loss and accuracy are obtained. Figure 5 and 6 given below shows the accuracy and loss percentage plot of both the training and validation set.

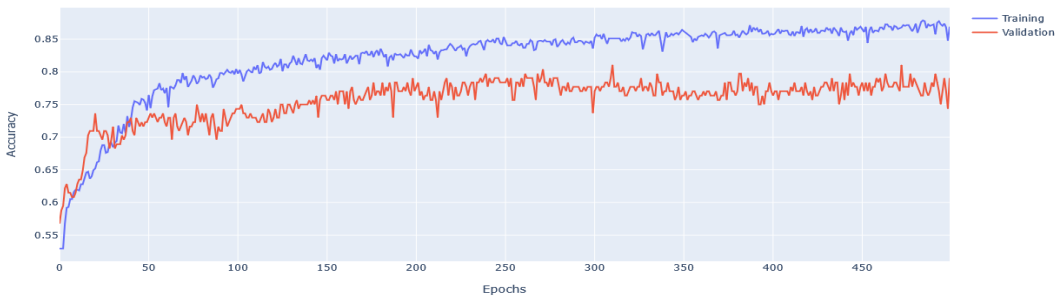

Fig.5 Accuracy percentage plot

Figure 5 given above shows the accuracy percentage plot of both the training sample and the validation sample for the first 500 epochs. The accuracy percentage of both the training sample and validation sample gradually increases through each epoch and the accuracy percentage of the training set remains higher than the validation set. During these epochs' duration, the training dataset was given a batch size of 32. In later stages of training, to get better accuracy dataset was trained further with different batch sizes (16, 64,128) and learning rates.

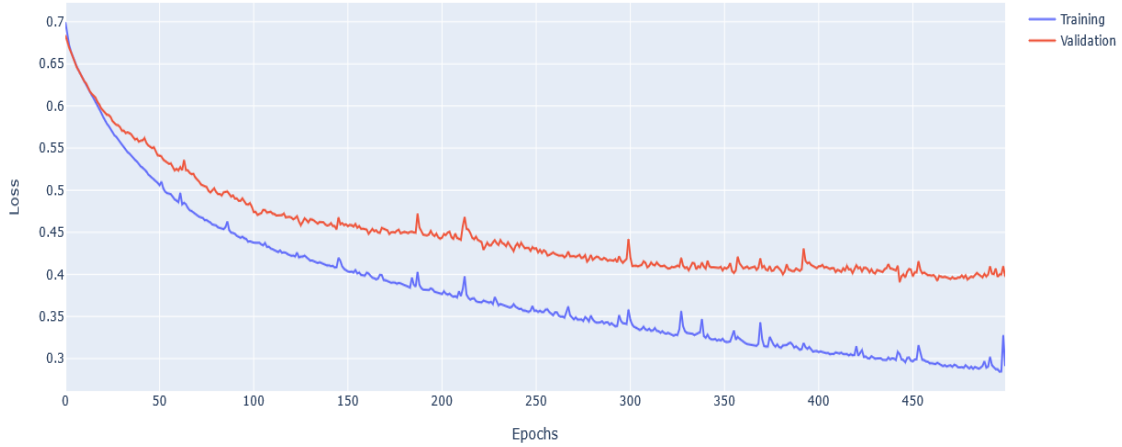

Fig.6 Loss percentage plot

Figure 6 given above shows the loss percentage plot of both the training sample and the validation sample for the first 500 epochs. The loss percentage of both the training set and validation set gradually decreases through each epoch and the loss percentage of the training set remains lower than the validation set.

IV. Results

This study aims to predict the presence of arthritis in IR thermal images using DL such as CNN. The dataset required for this work is collected in real-time using IR thermal camera. The collected image dataset consists of both normal and OA images. The dataset was split into two parts the training sample (85% of the total sample) and the validating sample (15% of the total sample). The dataset is then normalized and prepared to be analysed by the CNN model. The DL model is first trained using the training dataset and then validated using the validating dataset. Table 2 given below tabulates the performance analysis of the training and validation set.

Table.2 Performance analysis of training and validating set

Matrix	Training set	Validate set
Loss	0.14154645800590515	0.44490283727645874
Accuracy	0.9555822610855103	0.878378391265869
F1 Score	0.948289215564727	0.8745294809341431
Precision	0.9892035722732544	0.904166579246521

Recall	0.91307079792022	0.8516238927841187
Specificity	0.9543910622596741	0.9207056164741516

From table 1, the loss percentage of the training set is given as about 1.4% and for the validating set, it is about 4.4%. The accuracy of the training set is about 95.5% and for the validation set, it is about 87.8%. The F1 score of the training set is about 94.8% and the validation set is about 87.4%. The precision percentage of the training set is about 98.9% whereas the value of the validating set is about 90.4%. The recall value for the training set is about 91.3% and for the validation set, it is about 85.1%. The specificity value for the training set is about 95.4% and for the validation set, it is about 92%.

From the confusion matrix, the True positive value for the training sample is about 339 and for the validation sample, it is about 59. The True negative value is about 457 for the training sample and 71 for the validation sample. The False-positive value for the training sample is about 4 and for the validation sample, it is about 6. The False-negative value for the training sample is about 33 and 12 for the validation sample respectively. Table 3 given below shows the performance of each parameter on each class i.e., normal and arthritis-affected datasets.

Table.3 Performance in each class

	Precision	**Recall**	**F1-score**	**Support**
Normal	0.86	0.92	0.89	77
Arthritis	0.91	0.83	0.87	71

Table 3 given above shows the parametric values of both the Normal and Arthritis affected image dataset. The precision value for the Normal image dataset was about to 86% and for the Arthritis affected image dataset, it was about 91%. The recall value for the normal image dataset was about 92% and for the Arthritis affected image dataset, it was about 83%. The F1 score for the normal image dataset was about 89% and for the Arthritis affected image dataset, it was about 87%. The support value for the normal image dataset was about 77% and for the Arthritis affected image dataset, it was about 71%.

V. Optimization

The trained model requires very high memory and computation power. This is quantized to reduce memory and computation power using TensorFlow lite. The trained model is 38720 bytes which are very hard to fit into microcontrollers such as ARM Cortex M3 which generally have 64 Kilobytes of RAM. As a result, all N weights' floating-point precision has been lowered from 64 bits to 16/32 bits. The typical dataset is being used to prune parameters throughout model optimization, i.e., to reduce the dimensionality by systematic pruning. TensorFlow lite converts the model to Flat buffer format (.tflite), the flat buffer is converted into a C byte array in the form of a simple C file. The converted ".h" format file could be used in the embedded C program. The ".tflite" model can be deployed on Raspberry pi as well. This model can use additional computational resources like a Neural compute stick if present in Raspberry pi.

After Quantization the model size was reduced to 3832 bytes which are approximately 9.89% of the initial size. The size could be still reduced if the floating-point weights are converted to an integer, but the accuracy of the model becomes less in that case. Though the dataset is quantized and analysed using the DL model there is not much change in the output performance metrics. The loss percentage of the quantized model is higher compared to the trained model but the loss percentage is negligibly low and so it does not impact the performance metrics value much. Figure 7 given below shows the performance of the optimized model and raw model using the training set.

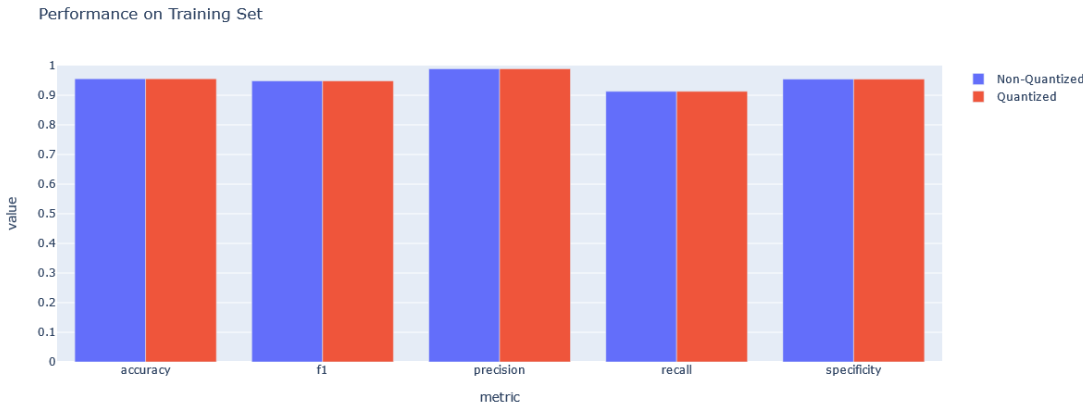

Fig.7 Performance of the optimized model and raw model using the training set

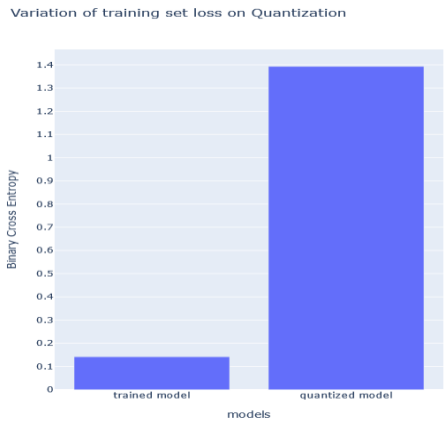

Fig.8 Variation of training set loss on quantization

Figure 8 given above shows the variation of loss percentage on the training set after quantization. It is given that the loss is less for the trained model and relatively for the quantized model. There is only an increase in the loss but the other matrices like F1, Accuracy, precision, recall, and specificity remain unchanged.

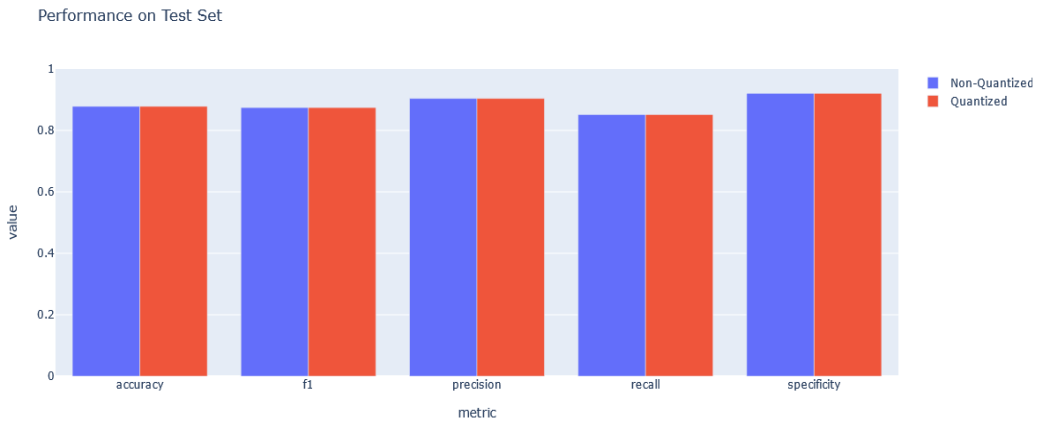

Fig.9 Performance of the optimized model and raw model using validating set

Figure 9 given above shows the performance of the optimized model and raw model using the validating set. There is only an increase in the loss but the other matrices like F1, Accuracy, precision, recall, and specificity remain unchanged.

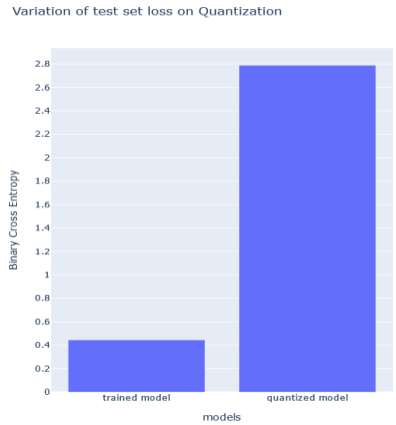

Fig.10 Variation of validating set loss on quantization

Figure 10 given above shows the variation of loss percentage on the validation set after quantization. It is given that the loss is less for the trained model and relatively for the quantized model.

VI. Conclusion

Pain, soreness, rigidity, and inflammation in and around one or many joints are common symptoms of Osteoarthritis conditions. There are several methods available to detect and diagnose arthritis such as CT, Ultrasound, MRI, Radiography, etc., but IR imagining is considered one of the most efficient and non-invasive methods. In this study, the dataset is collected using an IR camera in real-time. The collected dataset contains thermal images of both normal and arthritis-affected images. After that, the images are processed to make them compliant with the DL model. For the temperature value, statistically relevant metrics such as mean, median, mode, and so on are computed. The prepared data is then visualized to see the statistical parameter distributions graphically. The covariance matrix for the parameters is then calculated. After that, the data is pre-processed using the normalization method. The pre-

processed dataset is then separated into two parts: the training set, which accounts for 85% of the total dataset, and the validation set, which accounts for 15%. The CNN model is then trained and evaluated using the training and validation datasets, respectively. To analyse the efficiency of the model performance metrics of the model such as accuracy, precision, etc. are calculated. The accuracy of the model trained using the dataset is about 95.5%, which makes the model better and more efficient than the pre-existing models. The model is then quantized using the optimization method to reduce the complexity and computational time. A comparison between the loss percentage of the trained model and the quantized model is drawn. The loss percentage is slightly higher in the quantized model than in the trained model but the loss value is negligible hence it does not affect the models.

Ethics approval and consent to participate: This research did not contain any studies involving animal or direct human participants. No specific permissions were required for corresponding locations.

Consent for publication: The authors give their Consent to publish this work in the journal; we give our consent of publication to the publisher.

Availability of data and material: The authors declare that the required data and materials for this work is open source and can be used freely.

Funding: The authors declare that they do not have received funding for the work reported in this paper.

Competing interests: The authors declare that they have no conflict of interest.

Authors' contributions: Both the authors contributed in planning, conduct, execution of work and drafting / reporting of the work described in this paper.

Acknowledgement: The authors are grateful to all of those with whom they have had the pleasure to work during this research part.

REFERENCES

1. Woolf AD. “The bone and joint decade strategies to reduce the burden of disease: the Bone and Joint Monitor Project”. J Rheumatol Suppl; The Journal of Rheumatology, vol. 67, pp. 6-9, 2003.
2. Y. Nasser, R. Jennane, A. Chetouani, E. Lespessailles, and M. E. Hassouni, "Discriminative Regularized Auto-Encoder for Early Detection of Knee OsteoArthritis: Data from the Osteoarthritis Initiative," in IEEE Transactions on Medical Imaging, vol. 39, no. 9, pp. 2976-2984, Sept. 2020, doi: 10.1109/TMI.2020.2985861.
3. Dell'Isola, Andrea & Allan, Richard & Smith, Stephanie & Marreiros, Sara & Steultjens, Martijn. “Identification of clinical phenotypes in knee osteoarthritis: a systematic review of the literature”. BMC Musculoskeletal Disorders, vol. 17, 2016, 10.1186/s12891-016-1286-2.
4. Chaudhary, S. . (2022). On the Minimality of Leibniz Isomorphisms. International Journal on Recent Trends in Life Science and Mathematics, 9(1), 11–18. https://doi.org/10.17762/ijlsm.v9i1.137
5. Tins, B.J., Butler, R. “Imaging in rheumatology: reconciling radiology and rheumatology”. Insights Imaging, vol. 4, 2013, pp. 799–810, https://doi.org/10.1007/s13244-013-0293-1

6. Patil, Pravin & Dasgupta, Bhaskar. “Role of diagnostic ultrasound in the assessment of musculoskeletal diseases”, Therapeutic advances in musculoskeletal disease, vol. 4, 2012, pp. 341-55. 10.1177/1759720X12442112.
7. Narváez JA, Narváez J, De Lama E, De Albert M. “MR imaging of early rheumatoid arthritis”, Radiographics, Vol. 30, No. 1, pp. 143-63, 2010, doi: 10.1148/rg.301095089. PMID: 20083591.
8. Van der Heijde, D.M., “Assessment of radiographs in longitudinal observational studies”. The Journal of Rheumatology Supplement, vol. 69, 2004, pp.46-47.
9. U. Snekhalatha, M. Anburajan, T. Teena, B. Venkatraman, M. Menaka and B. Raj, "Thermal image analysis and segmentation of hand in evaluation of rheumatoid arthritis," 2012 International Conference on Computer Communication and Informatics, 2012, pp. 1-6, doi: 10.1109/ICCCI.2012.6158784.
10. M. S. Kiran and P. Yunusova, “Tree-Seed Programming for Modelling of Turkey Electricity Energy Demand”, Int J Intell Syst Appl Eng, vol. 10, no. 1, pp. 142–152, Mar. 2022.
11. Constance R Chu, Ashley A Williams, Christian H Coyle and Megan E Bowers, “Early diagnosis to enable early treatment of pre-osteoarthritis”, Arthritis Research & Therapy, pp. 14:212 , 2012, http://arthritis-research.com/content/14/3/212
12. J. Lee, J. Lee, S. Song, H. Lee, K. Lee and Y. Yoon, "Detection of suspicious pain regions on a digital infrared thermal image using the multimodal function optimization," 2008 30th Annual International Conference of the IEEE Engineering in Medicine and Biology Society, 2008, pp. 4055-4058, doi: 10.1109/IEMBS.2008.4650100.
13. Umapathy, Snekhalatha & Mariamichael, Anburajan & v, Sowmiya & Balasubramaniam, Venkatraman & Menaka, M. “Automated hand thermal image segmentation and feature extraction in the evaluation of rheumatoid arthritis”. Proceedings of the Institution of Mechanical Engineers. Part H, Journal of engineering in medicine, vol. 229, 2015, pp. 319-31, 10.1177/0954411915580809.
14. Sharon H, Elamvazuthi I, Lu C-K, Parasuraman S, Natarajan E. “Development of Rheumatoid Arthritis Classification from Electronic Image Sensor Using Ensemble Method”. Sensors, vol. 20, No. 1, 2020, https://doi.org/10.3390/s20010167
15. Varjú, G & Pieper, Carl & Renner, Jordan & Kraus, Virginia. “Assessment of hand osteoarthritis: Correlation between thermographic and radiographic methods”. Rheumatology (Oxford, England). vol. 43, pp. 915-9, 2004, 10.1093/rheumatology/keh204.
16. Jin, Chao & Yang, Yang & Xue, Z.-J & Liu, K.-M & Liu, Jing. “Automated Analysis Method for Screening Knee Osteoarthritis using Medical Infrared Thermography”. Journal of Medical and Biological Engineering, vol. 33, 2013, pp. 471-477, 10.5405/jmbe.1054.
17. Agarwal, D. A. . (2022). Advancing Privacy and Security of Internet of Things to Find Integrated Solutions. International Journal on Future Revolution in Computer Science &Amp; Communication Engineering, 8(2), 05–08. https://doi.org/10.17762/ijfrcsce.v8i2.2067
18. Ananthakrishnan, B., V. . Padmaja, S. . Nayagi, and V. . M. “Deep Neural Network Based Anomaly Detection for Real Time Video Surveillance”. International Journal on Recent and Innovation Trends in Computing and Communication, vol. 10, no. 4, Apr. 2022, pp. 54-64, doi:10.17762/ijritcc.v10i4.5534.

19. ElGohary, Sherif. “Thermal effect for optical imaging of knee osteoarthritis”. MOJ Applied Bionics and Biomechanics, vol. 3, 2019, 10.15406/mojabb.2019.03.00122.
20. Swati Wasnik, Vrishali Fulzele, Ishika Vora, Pankaj Khoabragade, Mrunal Raut, Md Waseem Khanooni, “Arthritis Prediction using Thermal Images and Neural Network”, International Research Journal of Engineering and Technology (IRJET), e-ISSN: 2395-0056 Vol. 07, Issue: 03, 2020
21. A. Kumar and P. Saxena, "Quantification of Cartilage loss for Automatic Detection and Classification of Osteoarthritis using Machine Learning approach," 2019 10th International Conference on Computing, Communication and Networking Technologies (ICCCNT), 2019, pp. 1-6, doi: 10.1109/ICCCNT45670.2019.8944538.
22. A. Alexos, C. Kokkotis, S. Moustakidis, E. Papageorgiou and D. Tsaopoulos, "Prediction of pain in knee osteoarthritis patients using machine learning: Data from Osteoarthritis Initiative," 2020 11th International Conference on Information, Intelligence, Systems and Applications (IISA, 2020, pp. 1-7, doi: 10.1109/IISA50023.2020.9284379.
23. Nouby M. Ghazaly, A. H. H. . (2022). A Review of Using Natural Gas in Internal Combustion Engines. International Journal on Recent Technologies in Mechanical and Electrical Engineering, 9(2), 07–12. https://doi.org/10.17762/ijrmee.v9i2.365
24. S. B. Kwon, H. -S. Han, M. C. Lee, H. C. Kim, Y. Ku and D. H. Ro, "Machine Learning-Based Automatic Classification of Knee Osteoarthritis Severity Using Gait Data and Radiographic Images," in IEEE Access, vol. 8, pp. 120597-120603, 2020, doi: 10.1109/ACCESS.2020.3006335.
25. Mohamed Yacin Sikkandar, S. Sabarunisha Begum, Abdulaziz A. Alkathiry, Mashhor Shlwan N. Alotaibi and Md Dilsad Manzar, “Automatic Detection and Classification of Human Knee Osteoarthritis Using Convolutional Neural Networks”, Computers, Materials & Continua, doi:10.32604/cmc.2022.020571
26. Mishra, Prabhaker & Pandey, ChandraM & Singh, Uttam & Gupta, Anshul & Sahu, Chinmoy & Keshri, Amit. “Descriptive Statistics and Normality Tests for Statistical Data”. Annals of Cardiac Anaesthesia, vol. 22, pp. 67-72, 2019, 10.4103/aca.ACA_157_18.
27. Singh, Dalwinder & Singh, Birmohan. “Investigating the impact of data normalization on classification performance”, Applied Soft Computing, vol. 105524, 2019, 10.1016/j.asoc.2019.105524.
28. Alzubaidi, L., Zhang, J., Humaidi, A.J. et al. “Review of deep learning: concepts, CNN architectures, challenges, applications, future directions”. J. Big Data, vol. 8, No. 53, 2021, https://doi.org/10.1186/s40537-021-00444-8
29. Sreelatha, T., Subramanyam, M.V. & Prasad, M.N.G. Early Detection of Skin Cancer Using Melanoma Segmentation technique. J Med Syst 43, 190 (2019). https://doi.org/10.1007/s10916-019-1334-1